




PSMC1 variant causes a novel neurological syndrome

Sarit Aharoni¹ | Regina Proskorovski-Ohayon¹ | Ramesh Kumar Krishnan² | Yuval Yogev¹  | Ohad Wormser¹ | Noam Hadar¹ | Anna Bakhrat² | Ismael Alshafee¹ | Maya Gombosh¹ | Nadav Agam¹ | Libe Gradstein³ | Zamir Shorer⁴ | Raz Zarivach² | Marina Eskin-Schwartz⁵  | Uri Abdu² | Ohad S. Birk^{1,5} 

¹The Morris Kahn Laboratory of Human Genetics, National Institute for Biotechnology in the Negev and Faculty of Health Sciences, Ben-Gurion University of the Negev, Beer Sheva, Israel

²Department of Life Sciences, Faculty of Natural Sciences, Ben-Gurion University of the Negev, Beer Sheva, Israel

³Department of Ophthalmology, Soroka University Medical Center and Clalit Health Services, Ben-Gurion University of the Negev, Beer-Sheva, Israel

⁴Pediatric Neurology Unit, Division of Pediatrics, Soroka Medical Center, Beer Sheva, Israel

⁵Genetics Institute, Soroka Medical Center, Ben-Gurion University of the Negev, Beer Sheva, Israel

Correspondence

Ohad S. Birk, Genetics Institute, Soroka Medical Center, Ben-Gurion University of the Negev, Beer Sheva, Israel.
Email: obirk@bgu.ac.il

Uri Abdu, Department of Life Sciences, Faculty of Natural Sciences, Ben-Gurion University of the Negev, Beer Sheva, Israel.
Email: abdu@bgu.ac.il

Funding information

Israel Science Foundation; Morris Kahn Family Foundation; National Knowledge Center for Rare/Orphan Diseases sponsored by the Israeli Ministry of Science, Technology and Space

Abstract

Proteasome 26S, the eukaryotic proteasome, serves as the machinery for cellular protein degradation. It is composed of the 20S core particle and one or two 19S regulatory particles, composed of a base and a lid. To date, several human diseases have been associated with mutations within the 26S proteasome subunits; only one of them affects a base subunit. We now delineate an autosomal recessive syndrome of failure to thrive, severe developmental delay and intellectual disability, spastic tetraplegia with central hypotonia, chorea, hearing loss, micropenis and undescended testes, as well as mild elevation of liver enzymes. None of the affected individuals achieved verbal communication or ambulation. Ventriculomegaly was evident on MRI. Homozygosity mapping combined with exome sequencing revealed a disease-associated p.I328T *PSMC1* variant. Protein modeling demonstrated that the *PSMC1* variant is located at the highly conserved putative ATP binding and hydrolysis domain, and is suggested to interrupt a hydrophobic core within the protein. Fruit flies in which we silenced the *Drosophila* ortholog *Rpt2* specifically in the eye exhibited an apparent phenotype that was highly rescued by the human wild-type *PSMC1*, yet only partly by the mutant *PSMC1*, proving the functional effect of the p.I328T disease-causing variant.

KEYWORDS

monogenic disease, neurological syndrome, proteasome 26S, protein homeostasis, *PSMC1*, *Rpt2*

Marina Eskin-Schwartz, Uri Abdu, and Ohad S. Birk contributed equally to this work.

This is an open access article under the terms of the [Creative Commons Attribution-NonCommercial-NoDerivs](https://creativecommons.org/licenses/by-nc-nd/4.0/) License, which permits use and distribution in any medium, provided the original work is properly cited, the use is non-commercial and no modifications or adaptations are made.

© 2022 The Authors. *Clinical Genetics* published by John Wiley & Sons Ltd.

1 | INTRODUCTION

Proteasomes are present in eukaryotes, archaea, and some of the bacteria.^{1,2} They serve as the machinery for protein degradation, a key component in protein homeostasis and turnover, and influence the regulation of most cellular processes.^{3–6} Proteasome 26S is the eukaryotic proteasome, composed of a 20S core particle (CP) and one or two 19S regulatory particles (RP), also known as PA700,^{7,8} which is highly conserved among eukaryotes and unique to them.¹ The 20S is a barrel-shaped catalytic core assembled from two identical inner rings consisting of seven different β subunits, as well as two identical outer rings consisting of seven α subunits.⁹ The proteolytic activity is carried out by three types of the β subunits, with caspase-like, trypsin-like, and chymotrypsin-like activity.¹⁰ RP consists of two subcomplexes, the base and the lid; both are composed of further subunits.^{5,10} The lid, whose principal activity is proposed to be deubiquitylation, is composed of nine non-ATPase subunits: PSMD3, PSMD6–PSMD9, and PSMD11–PSMD14.^{5,11,12} The base comprises six paralogous AAA+ ATPases (ATPases associated with diverse cellular activities) termed PSMC1–PSMC6 and three non-ATPases termed PSMD1/Rpn2, PSMD2/Rpn1, and ADRM/Rpn13; the last two function as a ubiquitin receptor. Another ubiquitin receptor is Rpn10, which is located between the lid and base.^{1,5} In brief, proteins are tagged by the polyubiquitin chain, which starts with ubiquitin activation by a ubiquitin-activating enzyme (also known as E1). Next, the activated ubiquitin is transferred to an ubiquitin carrier protein (E2) and finally transferred to the target protein by ubiquitin–protein ligase (E3).¹³ After the first ubiquitin attachment, the process continues to create a polyubiquitin chain upon the protein, while the attachment is usually on Lys48 of the previous ubiquitin.¹⁴ Proteins with a chain of at least four ubiquitins are delivered to the proteasome¹⁵ and bind directly to it by the ubiquitin receptors of the RP.¹⁶ Tagged proteins can also be introduced by adaptors that bind both the proteasome and the ubiquitin chain.¹⁷ The ubiquitinated protein undergoes deubiquitylation by PSMD14/ Rpn11.¹⁶ Next, the AAA+ ATPases ring motor engages with the initiation region of the substrate and, by the use of ATP hydrolysis, initiates unfolding and translocation toward the catalytic core,¹⁸ where it undergoes degradation into short peptide.¹⁶

To date, several human diseases have been associated with variants within the 26S proteasome subunits: chronic atypical neutrophilic dermatosis with lipodystrophy and elevated temperature (CANDLE) syndrome, known also as the proteasome-associated autoinflammatory syndrome (PRAAS), is an autoinflammatory disease characterized by early recurrent fever, nodular skin rashes, panniculitis-induced lipodystrophy, and multisystem inflammation.^{19,20} CANDLE has been shown to be associated with mutations in *PSMA3*, encoding the $\alpha 7$ subunit of the CP, in *PSMB8*, a gene member of the immunoproteasome, in *PSMB4*, as well as in *PSMB9* in a single patient. Most CANDLE patients described to date are homozygous or compound heterozygous for *PSMB8* mutations, but others are compound heterozygous for *PSMB4*, or are heterozygous for combinations such as *PSMA3/PSMB8*, *PSMB9/PSMB4*, or *PSMB8/PSMB4*.²⁰ In the latter situation, a digenic inheritance is suggested causing additive proteasome defects. Patients with digenic inheritance have variable proteolytic defects.²⁰ Biallelic mutations in

another component of the CP, *PSMB1*, of the $\beta 6$ subunit, have been associated with a neurodevelopmental disorder of microcephaly, intellectual disability, severe developmental delay and hypotonia.²¹ As for the RP, 10 individuals with de novo heterozygous loss-of-function genomic deletions or point mutations in *PSMD12* (encoding an RP lid subunit) were shown to have a syndrome of intellectual disability with congenital malformations, ophthalmologic anomalies, feeding difficulties, deafness, and subtle dysmorphic facial features.²² Only one of the base subunits of the RP has been associated with a human disease: a biallelic deep intronic variant with a predicted splicing effect in *PSMC3*, encoding one of the ATPase subunits, was shown to cause a neurosensory syndrome combining neurodevelopmental anomalies (autism, ataxia, mild intellectual disability) and mild facial dysmorphism, with early-onset deafness, cataracts, and subcutaneous deposits.²³ Here, through genetic and in vivo studies, we delineate a novel complex neurological syndrome caused by a missense variant in *PSMC1*, a member of the base unit of the RP of the proteasome.

2 | MATERIALS AND METHODS

2.1 | Clinical phenotyping

Twelve family members of consanguineous Bedouin kindred were studied. Clinical phenotyping was determined by an experienced team of senior pediatric neurologist, geneticist and endocrinologist. DNA samples were obtained following informed consent and approval of the Soroka Medical Center Internal Review Board (IRB).

2.2 | DNA extraction from whole blood

Blood samples (~10 ml in 0.1 EDTA 0.5 M pH 8) were obtained from patients and healthy family members. Total DNA was extracted from leukocytes of peripheral blood samples using the E.Z.N.A SQ blood DNA Extraction Kit (Omega, GA, USA) according to the manufacturer's instructions. DNA concentrations were determined by spectrophotometer at OD₂₆₀ and ran on 1% agarose gel in TBE to validate its integrity (expected to be ~20 kbs in size).

2.3 | RNA extraction and cDNA synthesis

Total RNA was extracted from whole-blood using GENzol™ Tri RNA Pure Kit (Geneaid Biotech Ltd.) according to the manufacturer's instructions. Single-stranded cDNA libraries were prepared using the Verso cDNA Synthesis Kit (Thermo Scientific).

2.4 | Linkage analysis

Genome-wide linkage analysis was performed for the whole family using single nucleotide polymorphism (SNPs) microarrays.

Illumina Omni Express Beadchip with >750K SNP loci per sample (Illumina, San Diego, CA, USA) was used. Homozygosity mapping analysis was carried out using Homozygosity-Mapper (<http://www.homozygositymapper.org>), and Multipoint Logarithm of Odds (LOD) score was calculated via SUPERLINK ONLINE SNP 1.1 (<https://cbl-hap.cs.technion.ac.il>).

2.5 | Whole exome sequencing

Whole exome sequencing (WES) trio analysis of the proband and his parents was performed by CeGat (Tübingen, Germany). Paired-end sequencing (2 × 100 bp) was performed using state-of-the-art Illumina NovaSeq6000 Sequencing Systems (San Diego, CA). Data were analyzed using QIAGEN's Ingenuity Variant Analysis software (www.qiagen.com/ingenuity, QIAGEN, USA). We excluded common variants with an observed allele frequency of more than 0.5% in 1000 Genomes Project (<http://www.internationalgenome.org>), genome Aggregation Database (gnomAD) (<https://gnomad.broadinstitute.org>), the Allele Frequency Community (AFC), or variants appearing in a homozygous state in our in-house WES database of 553 controls. We then proceeded to filtration by keeping the predicted deleterious variants, as listed in HGMD[®] or ClinVar, classified as a disease associated (pathogenic or likely pathogenic) according to computed American College of Medical Genetics and Genomics (ACMG) guidelines classification or associated with loss-of-function of a gene (by causing frameshift, in-frame indel, start/stop codon change, missense, or splice site loss up to as predicted by MaxEntScan). All variants appearing in a homozygous state in the proband and a heterozygous state in his parents were selected. Those remaining variants were first prioritized using the functional annotations and were then further filtered based on the relevant genomic location, as determined by the linkage analysis. For verification of the variants, we used the BAM file loaded on the Integrative Genomics Viewer (IGV),²⁴ enabling direct visualization of the variants.

2.6 | Segregation and variant screening

Segregation analysis within the family and screening of 84 ethnically matched controls of the *PSMC1* variant were done by restriction fragment length polymorphism (RFLP) analysis using genomic DNA. The *PSMC1* variant region was amplified using PCR primers: forward 5'-ATCAGTTGAGTCTTCATTCCTCC-3' and reverse 5'-AAGCAGCAAGTTCTTGAGG-3', producing a 462 bp fragment. Restriction analysis was done using the NcoI-HF enzyme (New England Biolabs), based on a restriction site-specific to the variant yet not the wild-type sequence: the mutant (MUT) allele yielded two fragments, 318 and 144 bp, while the wild-type allele remained uncut. To further validate segregation of the *PSMC1* variant within the affected kindred, Sanger sequencing was performed using cDNA of the proband, his parents, and unaffected control, as an intronic indel SNP adjacent to the variant (rs71117332) was disrupting the clarity of the sequencing. Amplification of the variant was performed using the following

primers: forward 5'-TTCTCTATGGTCCACCTGG-3' and reverse 5'-AACTCAATCTTCCTGTCAATGC-3', generating a 391 bp amplicon.

2.7 | Multiple sequence alignment

Ortholog of *PSMC1* were identified using HomoloGene by NCBI (<https://www.ncbi.nlm.nih.gov/homologene>), and multiple sequence alignment (MSA) was performed by Clustal Omega (<https://www.ebi.ac.uk/Tools/msa/clustalo/>) with the following RefSeq sequence accession number: *Homo sapiens*; NP_002793.2, *Mus musculus*; NP_032973.1, *Drosophila melanogaster*; NP_524469.2, *Caenorhabditis elegans*; NP_504558.1, *Arabidopsis thaliana*; NP_179604.1, *Oryza sativa*; NP_001060719.1, and *Saccharomyces cerevisiae*; NP_010277.1. Identity was calculated via the Basic Local Alignment Search Tool (BLAST) (<https://blast.ncbi.nlm.nih.gov/Blast.cgi>).

2.8 | Protein modeling

NP_002793.2 was used for modeling *PSMC1*. Domains were identified using InterPro (www.ebi.ac.uk/interpro/) and a schematic protein model was generated using prosite (<https://prosite.expasy.org/mydomains/>). Prediction of protein structure was performed via PyMOL using Protein Data Bank (PDB) ID 6MSB (<https://www.rcsb.org/structure/6MSB>).

2.9 | Cloning and generation of transgenic flies

In order to generate pUAS-*PSMC1* constructs, first, the entire coding region of *PSMC1* (NM_001330212.2) was amplified from the proband and WT control, using the following primers: forward 5'-ATGAGGAA-GAATTCATTAGAAATCAGG-3' and reverse 5'-TTAGAGATACAGCCCTCAGGGGTGC-3'. The amplicon was cloned into pJET vector and sequenced for validation. For insertion in to pUAS-attB, it was linearized by digestion with XbaI and EcoRI enzymes (New England Biolabs). *PSMC1* WT and MUT were amplified from pJET-*PSMC1* using forward 5'-AAGAGAACTCTGAATAGGGAATTGGGAATTCATGGAGGAAGAATTCATTAGAAATCAGG-3' and reverse 5'-AAGTAAGGTTCCCTCACAAA-GATCCTCTAGATTAGAGATACAGCCCTCAGGGGTGC-3', followed by Gibson assembly. To ensure similar expression level, 3rd chromosome attP docking site (P{CaryP}attP2) for phiC31 integrase-mediated transformation was used for generating transgenic flies. P-element-mediated germline transformation of these constructs was carried out by BestGene (Chino Hills, CA, USA).

2.10 | Drosophila stocks

The following transgenic flies were used: RNAi-*Rpt2* (the fly ortholog of *PSMC1*) (Vienna *Drosophila* RNAi Center; V22052). M{UAS-βTub60D.ORF}ZH-86Fb was used as a transgenic fly control.²⁵

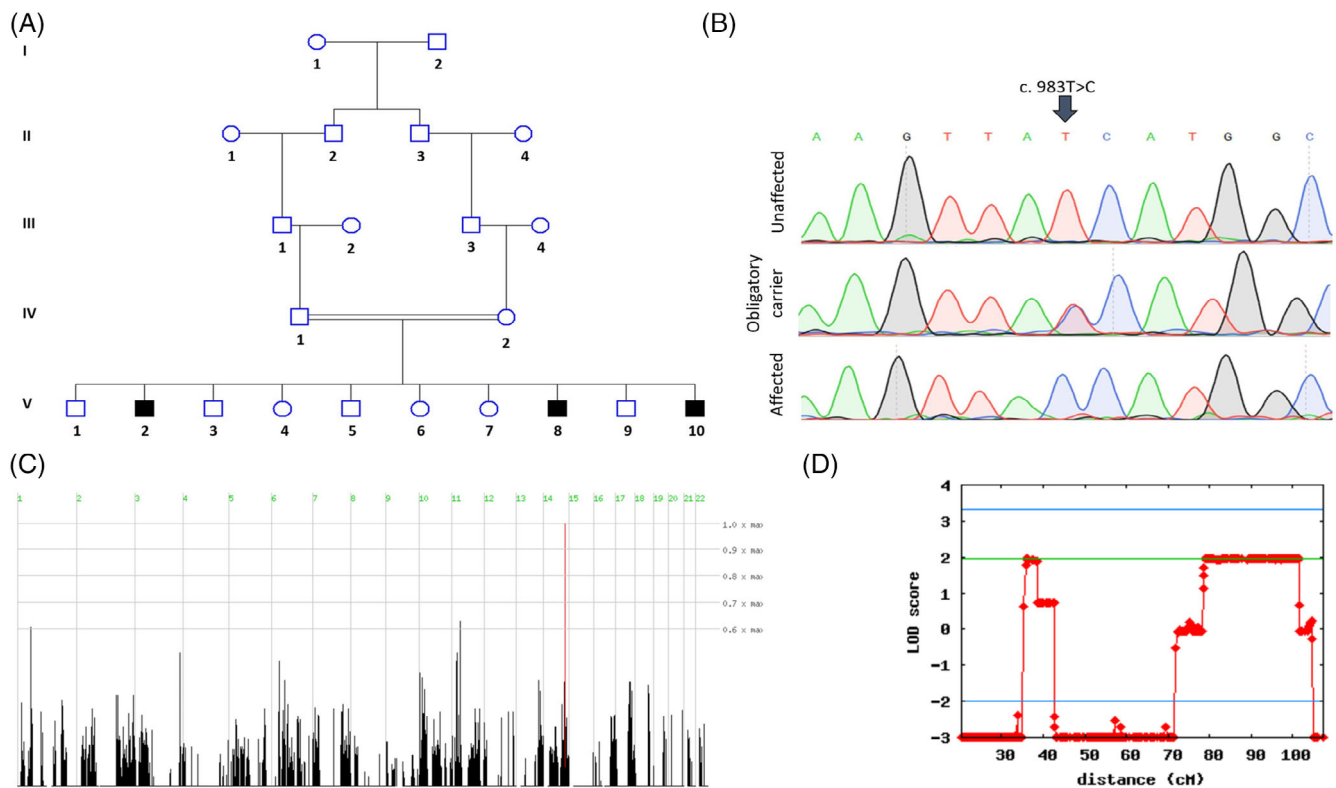


FIGURE 1 Pedigree, linkage analysis, and *PSMC1* variant. (A) Pedigree of the Bedouin studied kindred. Affected individuals are marked in black. (B) Sanger sequencing demonstrating the c.983T>C, p.I328T *PSMC1* missense variant: unaffected individual (V:1), obligatory carrier (IV:1), and affected individual (V:2). (C) Homozygosity Mapper plot showing single homozygosity locus shared by affected individuals, marked in red. (D) LOD score analysis plot of chromosome 14 [Colour figure can be viewed at wileyonlinelibrary.com]

Eye expression was induced under the control of GMR-Gal4 driver. Follicle cell expression was induced under the control of traffic jam-(tj) Gal4. The Gal4 lines were obtained from the Bloomington Stock Center.

2.11 | Scanning electron microscope

Zero- and five-day *Drosophila* flies were fixed and dehydrated by immersing them in increasing ethanol concentrations (30%, 70%, and twice in 100%; 10 min each). The flies were then completely dehydrated using increasing hexamethyldisilazane (HMDS) concentrations in ethanol (30%, 70%, and twice in 100%; 90 min each). The samples were air-dried overnight, placed on stubs, and coated with gold. The specimens were examined with a scanning electron microscope (SEM; Verios XHR 460 L).

3 | RESULTS

3.1 | Clinical phenotyping and laboratory investigations

Twelve family members of consanguineous Bedouin kindred were studied. Clinical phenotyping was determined by an experienced team of

senior pediatric neurologist, geneticist and endocrinologist. DNA samples were obtained following informed consent and approval of the Soroka Medical Center Internal Review Board (IRB). Three of the 10 offspring of healthy consanguineous parents of Bedouin Israeli ancestry (Figure 1A) were affected with a similar phenotype of failure to thrive, developmental delay and severe intellectual disability, spastic tetraplegia with central hypotonia, chorea, as well as hearing loss (details in Table 1). None of the three achieved verbal communication or ambulation (sitting / standing) at any age. They had mild dysmorphism of borderline dolichocephaly and microcephaly, prominent bushy eyebrows, flat midface, long nasal bridge and micrognathia. All three had micropenis with undescended testes. V10 (as a toddler) underwent thorough endocrinological analysis: testosterone and gonadotropin levels were low. Evaluation of other anterior pituitary hormone axes revealed no abnormalities. Karyotype and SRY were normal. All three affected subjects had mild-to-moderate macrocytic anemia. B12, folic acid and TSH levels were normal. Two of the affected individuals (V10, V2) had cholestatic jaundice that resolved within months after birth, with residual persistent augmented liver enzyme blood levels. Otherwise, blood chemistry was normal. One individual (V10) had a duplicated renal collecting system and a muscular ventricular septal defect, which might not be related to the *PSMC1* mutation. Brain MRI (V10 as a toddler; V2 at early adolescence) was normal except for global mild to moderate ventriculomegaly and broadened extra-axial space. Notably, pituitary

TABLE 1 Disease phenotype of affected individuals

Patient	V-2	V-8	V-10
Age at last exam (years)	20	8	3
Verbal communication	–	–	–
Ambulation (ability to sit / stand)	–	–	–
Chorea	n/a	+	+
Hearing loss	+	+	+
Visual tracking	–	+	+
Spastic tetraplegia with central hypotonia	+	+	+
Knee reflexes	–	–	–
Babinski sign	Negative	Negative	Negative
Micropenis	+	+	+
Undescended testes	+	+	+
Mild dysmorphism	+(Mostly evident at earlier age)	+	+
Cholestatic jaundice that resolved within months after birth, with residual persistent augmented liver enzyme blood levels	+	–	+
Feeding through PEG	+	+	–
Duplicated renal collecting system and a muscular ventricular septal defect	–	–	+

Abbreviations: n/a, data not available; PEG, percutaneous endoscopic gastrostomy.

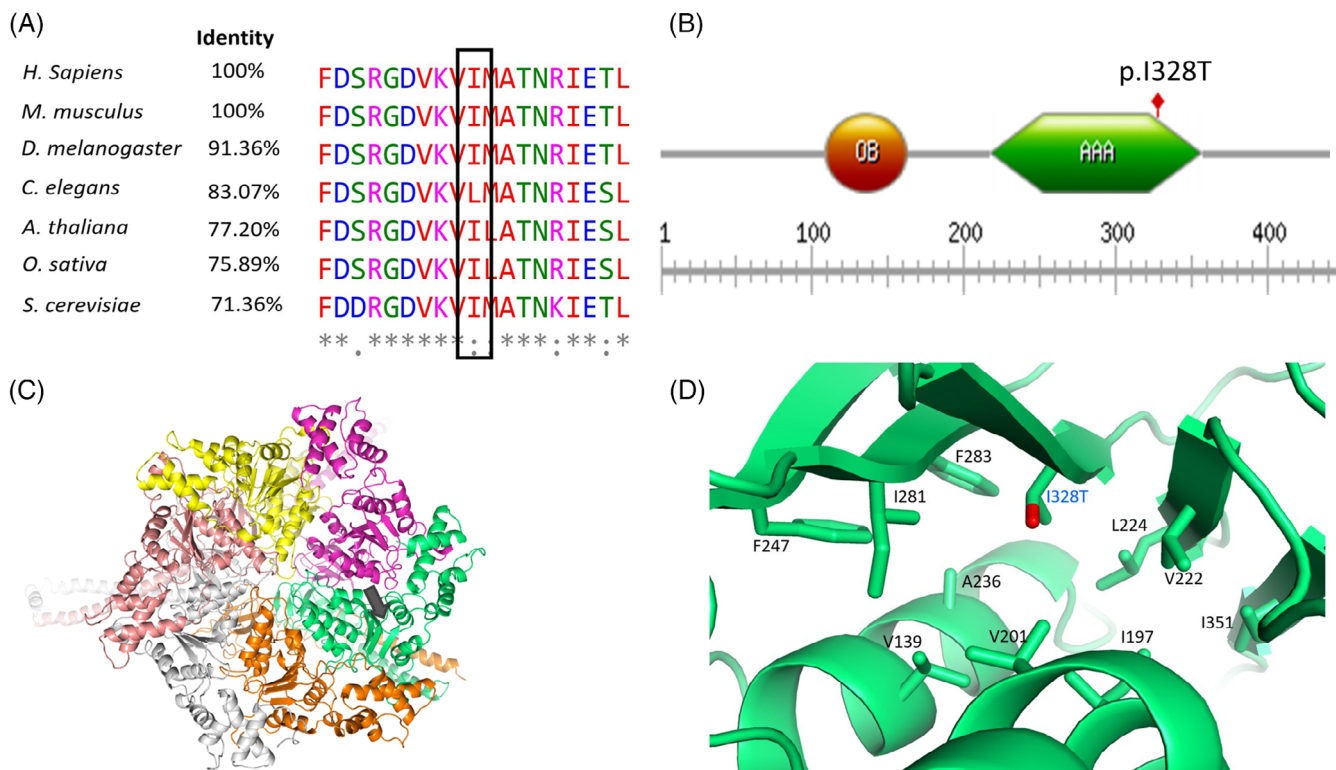


FIGURE 2 PSMC1 conservation and structure. (A) Protein multiple sequence alignment (MSA) for PSMC1. Black rectangle marks the p.I328 isoleucine residue. (B) Schematic model of PSMC1. In orange, an oligonucleotide binding (OB) domain, in green AAA+ motor domain (AAA). Red flag marks the location of the amino acid substitution. (C) Structure of the PSMC ring of the regulatory particle (19S). PSMC1 is marked in green. Gray arrow indicates on the hydrophobic core, where the substitution is located. (D) Zoom-in on the hydrophobic core. The p.I328T substitution of isoleucine to threonine is labeled in blue; oxygen is marked in red [Colour figure can be viewed at wileyonlinelibrary.com]

structure was normal. EEG was normal. The eldest affected individual (V2), last examined at 20 years of age, had severe intellectual disability with no verbal contact or comprehension, spastic quadriplegia, and was fully nonambulatory, fed through gastrostomy, with severe failure to thrive (weight 13 kg). Blood chemistry was normal with borderline mildly elevated liver enzymes.

3.2 | Genetic analysis

Karyotype, SRY sequencing, and chromosomal microarray analysis of the proband (V10) were normal (data not shown). Genome-wide linkage analysis for all 12 family members identified a single ~1.14 Mb homozygous segment shared exclusively by all affected individuals (Figure 1A). The disease-associated haplotype of a chromosome 14 locus between SNPs rs10083415 and rs1286459 (positioned, respectively, at 89464163 and 90608806 in the GRCh38/Hg38 assembly), segregated within the family as expected for autosomal recessive heredity. The maximal multipoint LOD score for the pedigree was 1.95 (Figure 1D). Only two rare homozygous variants were found in this locus: in *TTC7B* and in *PSMC1*. The *TTC7B* variant (rs145554922;

NM_001010854.2, c.2416G>A, p.E721K) is predicted by PolyPhen-2²⁶ as benign and tolerated by SIFT.²⁶ Furthermore, this variant had a prevalence of 1.266% in our in-house WES control database and was found in a homozygous state in a control not affected with a similar phenotype. Thus, this variant was ruled out. The *PSMC1* variant (NM_001330212.1, c.764T>C, p.I255T / NM_002802.3, c.983T>C, p.I328T) was predicted as damaging and possibly damaging by SIFT²⁶ and by PolyPhen-2,²⁷ respectively. The variant was not found in our 553 WES database (mainly of the Bedouin community) nor in public databases (1000 Genomes, gnomAD, and AFC). The missense variant in *PSMC1* was demonstrated via RFLP and Sanger sequencing to fully segregate within the family as expected for recessive heredity (Figure 1B). Screening of 84 nonaffected individuals belonging to the same tribe of this family was performed by RFLP and did not identify any homozygous or heterozygous carriers of the *PSMC1* variant.

3.3 | Conservation and modeling

PSMC1 (transcript variant 1: NM_002802.3) encodes a 440 amino acid protein (NP_002793.2) which is highly conserved throughout

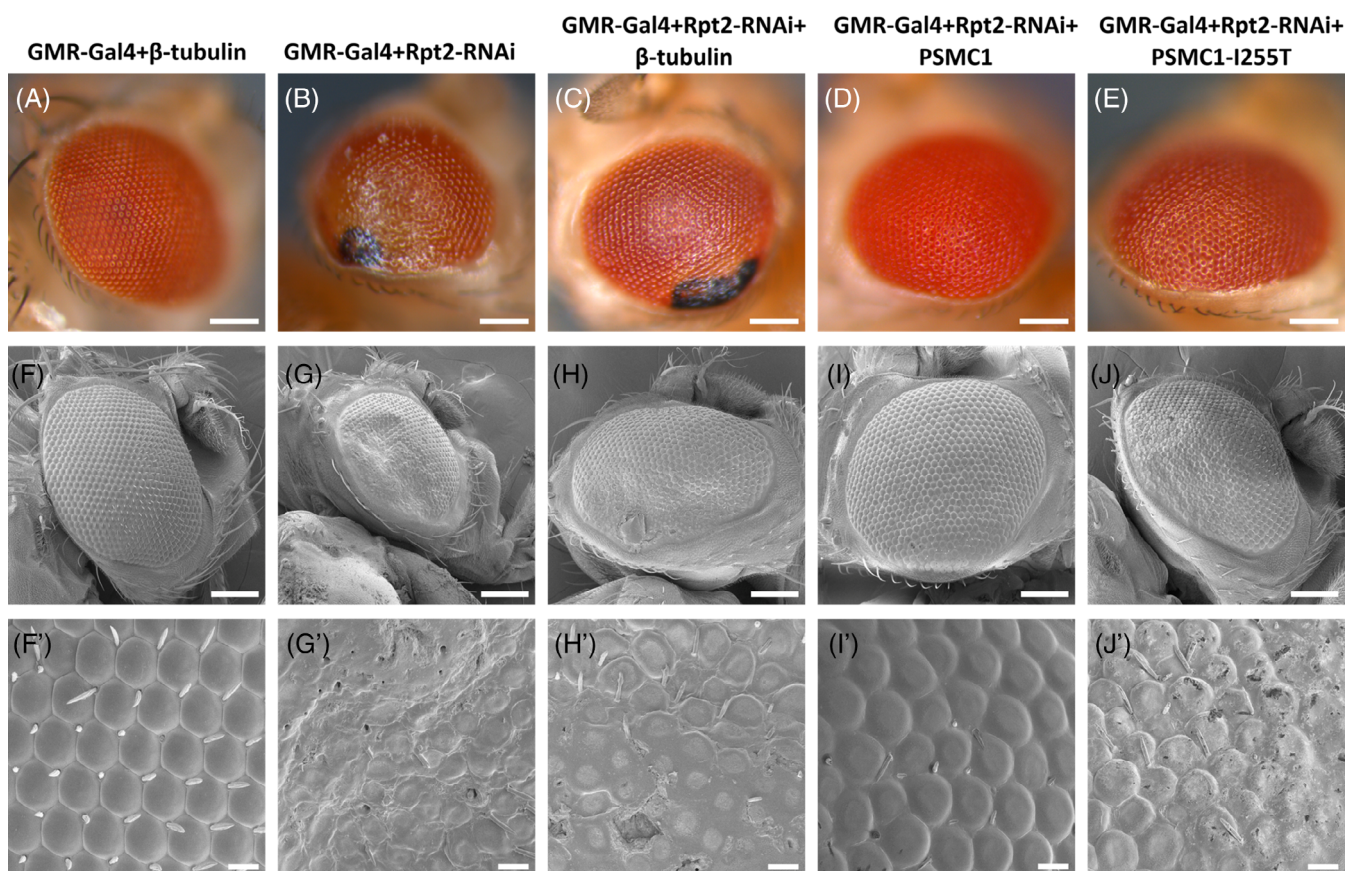


FIGURE 3 In vivo *Drosophila* assay. (A–E) Representative bright-field microscope images of fly eyes displaying eye-specific expression of GMR-Gal4 in the presence of pUAS β -tubulin-60D (A, F, F'), RNAi-*Rpt2* (B, G, G'), pUAS β -tubulin-60D and RNAi-*Rpt2* (C, H, H'), RNAi-*Rpt2* and *PSMC1*-WT (D, I, I'), and RNAi-*Rpt2* and *PSMC1*-I255T (E, J, J') from flies collected on zero day (same day of hatching). Black spots indicate necrotic areas and light areas indicate depigmentation. Bars of the whole fly eye represents 100 μ m. Zoom-in bars represent 10 μ m. [Colour figure can be viewed at wileyonlinelibrary.com]

evolution, all the way to *O. sativa* and *S. cerevisiae* (Figure 2A). The PSMC1 variant is located at the AAA-ATPase domain (Figure 2B), the putative ATP binding site, and the highly conserved region within the ATPases family.²⁸ The PSMC1 p.I328T missense variant is suggested to interrupt a hydrophobic core within the protein (Figure 2C, D). Missense Z score is 3.95 ($o/e = 0.28$; max score 5) and pLI = 1 ($o/e = 0.14$; pLI ≥ 0.9 considered to be extremely intolerant), with only five LoF variants, none homozygous, reported to date by gnomAD²⁹ (for ENST00000261303.8).

3.4 | In vivo *Drosophila* rescue experiments

PSMC1 is highly conserved across evolution, with 91.36% identity between the human and *D. melanogaster* ortholog protein, *Rpt2* (Figure 2A). Knock-out of the *PSMC1* ortholog in mice was shown to be embryonic lethal.³⁰ Similarly, silencing the *Drosophila* *PSMC1* ortholog, *Rpt2*, pan-neuronally, resulted in larvae not completing pupation.³¹ Utilizing a UAS-Gal4 tissue-specific knock-down system, Fernández-Cruz et al.³¹ have shown that expressing *Rpt2*-RNAi under a GMR-Gal4 driver resulted in eye degeneration with severe depigmentation and necrosis. We aimed to assess the ability of the wild type and mutant (p.I255T) human *PSMC1* to rescue the eye phenotype generated by *Rpt2* silencing in *Drosophila*. As there is significant divergence between the human construct and the RNAi, there was no risk of the RNAi targeting the human transgene.³² To that end, we generated transgenic flies carrying pUAS-PSMC1 or pUAS-PSMC1-I255T. Validation of transgenic gene expression in flies was performed by immunohistochemistry using ovaries from transgenic pUAS-PSMC1 flies, both WT and MUT, under TJ-Gal4 (traffic-jam-Gal4): both WT and MUT constructs expressed PSMC1 as expected in the follicle cells. Next, we generated fly stocks carrying both pUAS-*Rpt2*-RNAi and either pUAS-PSMC1 or pUAS-PSMC1-I255T. As control, we also generated transgenic flies carrying both *Rpt2*-RNAi and another unrelated pUAS construct (UAS- β Tub60D) (Figure 3C, H, H'). Silencing *Rpt2* specifically in the eye using GMR-Gal4 resulted in a severe eye phenotype, including depigmentation, necrosis, disorganization of ommatidia, fusion of ommatidia, irregularity of ommatidia shape and size, and loss of interommatidial bristles (Figure 3B, G, G'). While depigmentation and necrosis were fully rescued by both the wildtype and mutant human *PSMC1* constructs (Figure 3D, E), other characteristics of the ommatidia that were affected by *Rpt2* silencing were nearly fully rescued only with PSMC1-WT (Figure 3I, I'); expression of PSMC1-MUT failed to rescue fusion of ommatidia and extended ommatidia defects and anomalies (Figure 3J, J').

4 | DISCUSSION

We describe a novel autosomal recessive neurological syndrome of severe developmental delay with spastic paraplegia, chorea, micropenis, and mild dysmorphism. Through homozygosity mapping and WES, we demonstrated that the disease is caused by a *PSMC1* variant that

fully segregated within the family as expected for recessive heredity and was not found in ethnically matched controls. The disease phenotype is different from the CANDLE syndrome seen with mutations in *PSMA3*, *PSMB4*, *PSMB8*, and *PSMB9* encoding components of the CP,²⁰ yet significantly overlaps the phenotype seen in mutations of another component of the CP, *PSMB1*, of the $\beta 6$ subunit, causing a neurodevelopmental disorder of microcephaly, intellectual disability, severe developmental delay and hypotonia. The disease phenotype we describe also overlaps with that seen with dominant mutations in *PSMD12* (encoding a proteasome RP lid subunit), causing intellectual disability with congenital malformations, feeding difficulties, deafness, and subtle dysmorphic facial features.²² Most notably, major overlap is seen with the only disease reported to date due to another component of a base subunit of the RP: a biallelic variant in *PSMC3*, encoding one of the ATPase subunits, causing a neurosensory syndrome combining neurodevelopmental anomalies (autism, ataxia, mild intellectual disability) and mild facial dysmorphism, with early-onset deafness.²³ The ambiguous genitalia with micropenis, undescended testes and low testosterone levels seen with the *PSMC1* variant is unique and has not been reported in any of the diseases due to mutations in components of the proteasome.

PSMC1 encodes one of the ATPase subunits of the 19S RP of the 26S proteasome³³ and shows high conservation across evolution with intolerance for variation and loss of function, as indicated by the high Z score and pLI. The proteasome function is crucial for protein homeostasis and, therefore, influences most cellular pathways³⁴; its activity has been tied to neurogenesis³⁵ and angiogenesis.³⁶ Each ATPase includes an N-terminal helix, an oligonucleotide binding (OB) domain, and a C-terminal AAA+ motor domain.¹⁸ It is proposed that one of the leading forces that determine protein structure is hydrophobic side chains, which usually collapse into each other and are buried within the folded protein, hydrophobic core.^{37–39} The p.I328, mutated in the affected individuals, is part of the hydrophobic core of PSMC1; therefore, it is expected that its substitution by the hydrophilic threonine will affect the collapse of the core and, as a result, the structure of the protein.

To further delineate the effect of the variant on developmental processes, we reverted to *Drosophila*, studying its *PSMC1* ortholog, *Rpt2*. PSMC1 is ubiquitously and highly expressed throughout embryogenesis. Indeed, in a *C. elegans* RNAi silencing experiment it has been shown that knock-down of *Rpt2* at all larval stages and in adults causes lethality, demonstrating the indispensability of *Rpt2*/PSMC1 during embryogenesis and postembryonic development.⁴⁰ We thus generated flies in which we silenced *Rpt2* specifically in the eye. The resulting phenotype was almost fully rescued by the human wild-type *PSMC1* yet only partly by the mutant *PSMC1*, further proving the functional effect of the p.I328T variant.

Several studies have shown association of the ubiquitin-proteasome system (UPS) with neurodegeneration.^{10,41} *PSMC1* conditional knock-out mice exhibited 26S proteasome depletion and Lewy-like inclusions,³⁰ while *PSMC1* heterozygous knock-out mice did not show any effects on the mouse brain (yet their embryonic fibroblasts did show decreasing levels of *PSMC1* and cell cycle arrest).⁴² In quest of possible association between *PSMC1* and Parkinson diseases,

Fernández-Cruz et al.³¹ have shown that following *Rpt2* knock-down in the *D. melanogaster* central nervous system (CNS) under Elav-Gal4 driver and thermosensitive Gal80, proteasome activity was reduced, and augmentation of insoluble ubiquitinated protein was observed.

Notably, previous studies have tested possible association of *PSMC1* with human diseases: a clinical report of a heterozygous deletion of varying segments of a 14q32.11 locus with an overlapping deletion of *KCNK13*, *PSMC1*, *NRDE2*, *CALM1*, *TTC7B*, and *RPS6KA5* was associated with developmental and speech acquisition delays in three unrelated patients. However, one of the patients' mother tested positive for heroin at delivery and had with a history of heroin and tobacco use in previous pregnancies, and the nonaffected mother of another affected individual shared the heterozygous deletion of her affected son. No further genetic studies have been done on those patients.⁴³ Thus, in line with the lack of abnormal phenotype in the obligatory carrier parents in the kindred we describe, it is extremely likely that heterozygous loss of function of *PSMC1* results in no discernible phenotype in humans. Also notable is a study of possible association between variation in *PSMC1* and Parkinson disease, identifying no unique variation in *PSMC1* in Parkinson disease patients.⁴⁴ Interestingly, our patients share similar clinical features (e.g., intellectual disability, dysmorphism, hearing loss) with other disorders involving genes encoding proteasome RP subunits,^{22,23} probably reflecting common molecular mechanisms underlying these disorders. Nevertheless, our study is the first to clearly delineate a role of *PSMC1* in a human disease.

ACKNOWLEDGEMENTS

The authors thank the family for participating in this study.

CONFLICT OF INTEREST

The authors declare that they have no conflict of interest.

DATA AVAILABILITY STATEMENT

Data and material are available upon request to the corresponding authors.

ORCID

Yuval Yogev  <https://orcid.org/0000-0002-2218-9938>

Marina Eskin-Schwartz  <https://orcid.org/0000-0003-0507-1505>

Ohad S. Birk  <https://orcid.org/0000-0003-1430-1296>

REFERENCES

- Budenholzer L, Cheng CL, Li Y, Hochstrasser M. Proteasome structure and assembly. *J Mol Biol.* 2017;429(22):3500-3524. doi:10.1016/J.JMB.2017.05.027
- Humbarad MA, Maupin-Furlow JA. Prokaryotic proteasomes: nano-compartments of degradation. *Microb Physiol.* 2013;23(4-5):321-334. doi:10.1159/000351348
- Maupin-Furlow JA, Gil MA, Karadzic IM, Kirkland PA, Reuter CJ. Proteasomes: perspectives from the archaea. *Front Biosci.* 2004;9:1743.
- Coux O, Tanaka K, Goldberg AL. Structure and functions of the 20S and 26S proteasomes. *Annu Rev Biochem.* 2003;65:801-847. doi:10.1146/ANNUREV.BI.65.070196.004101
- Bard JAM, Goodall EA, Greene ER, Jonsson E, Dong KC, Martin A. Structure and function of the 26S proteasome. *Annu Rev Biochem.* 2018;87:697-724. doi:10.1146/annurev-biochem.2018.87.697-724
- Da Fonseca PCA, He J, Morris EP. Molecular model of the human 26S proteasome. *Mol Cell.* 2012;46(1):54-66. doi:10.1016/J.MOLCEL.2012.03.026
- Dahlmann B, Ruppert T, Kuehn L, Merforth S, Kloetzel PM. Different proteasome subtypes in a single tissue exhibit different enzymatic properties. *J Mol Biol.* 2000;303(5):643-653. doi:10.1006/JMBI.2000.4185
- Groll M, Huber R. Substrate access and processing by the 20S proteasome core particle. *Int J Biochem Cell Biol.* 2003;35(5):606-616. doi:10.1016/S1357-2725(02)00390-4
- Fort P, Kajava AV, Delsuc F, Coux O. Evolution of proteasome regulators in eukaryotes. *Genome Biol Evol.* 2015;7(5):1363-1379. doi:10.1093/GBE/EVV068
- Sahara K, Kogleck L, Yashiroda H, Murata S. The mechanism for molecular assembly of the proteasome. *Adv Biol Regul.* 2014;54(1):51-58. doi:10.1016/J.JBIOR.2013.09.010
- Sharon M, Taverner T, Ambroggio XI, Deshaies RJ, Robinson CV. Structural organization of the 19S proteasome lid: Insights from MS of intact complexes. *PLoS Biol.* 2006;4(8):e267. doi:10.1371/JOURNAL.PBIO.0040267
- Lander GC, Martin A, Nogales E. The proteasome under the microscope: the regulatory particle in focus. *Curr Opin Struct Biol.* 2013;23(2):243-251. doi:10.1016/J.SBI.2013.02.004
- Ciechanover A. Proteolysis: from the lysosome to ubiquitin and the proteasome. *Nat Rev Mol Cell Biol.* 2005;6(1):79-87. doi:10.1038/nrm1552
- Hershko A, Ciechanover A. The ubiquitin system. *Annu Rev Biochem.* 1998;67:425-479. Accessed August 17, 2021. www.annualreviews.org
- Bedford L, Paine S, Sheppard PW, Mayer RJ, Roelofs J. Assembly, structure, and function of the 26S proteasome. *Trends Cell Biol.* 2010;20(7):391-401. doi:10.1016/J.TCB.2010.03.007
- Ehlinger A, Walters KJ. Structural insights into proteasome activation by the 19S regulatory particle. *Biochemistry.* 2013;52(21):3618-3628. doi:10.1021/BI400417A
- Schrader EK, Harstad KG, Matouschek A. Targeting proteins for degradation. *Nat Chem Biol.* 2009;5(11):815-822. doi:10.1038/nchembio.250
- De La Peña AH, Goodall EA, Gates SN, Lander GC, Martin A. Substrate-engaged 26S proteasome structures reveal mechanisms for ATP-hydrolysis-driven translocation. *Science.* 2018;362(6418):eaav0725. doi:10.1126/SCIENCE.AAV0725
- Brehm A, Liu Y, Sheikh A, et al. Additive loss-of-function proteasome subunit mutations in CANDLE/PRAAS patients promote type I IFN production. *J Clin Invest.* 2015;125(11):4196-4211. doi:10.1172/JCI81260
- Torrello A. CANDLe syndrome as a paradigm of proteasome-related autoinflammation. *Front Immunol.* 2017;8(AUG):927. doi:10.3389/FIMMU.2017.00927/BIBTEX
- Ansar M, Ebstein F, Özkoç H, et al. Biallelic variants in *PSMB1* encoding the proteasome subunit $\beta 6$ cause impairment of proteasome function, microcephaly, intellectual disability, developmental delay and short stature. *Hum Mol Genet.* 2020;29(7):1132-1143. doi:10.1093/HMG/DDAA032
- Küry S, Besnard T, Ebstein F, et al. De novo disruption of the proteasome regulatory subunit *PSMD12* causes a syndromic neurodevelopmental disorder. *Am J Hum Genet.* 2017;100(2):352-363. doi:10.1016/J.AJHG.2017.01.003
- Kröll-Hermi A, Ebstein F, Stoetzel C, et al. Proteasome subunit *PSMC3* variants cause neurosensory syndrome combining deafness and cataract due to proteotoxic stress. *EMBO Mol Med.* 2020;12(7):e11861. doi:10.15252/EMMM.201911861
- Thorvaldsdóttir H, Robinson JT, Mesirov JP. Integrative genomics viewer (IGV): high-performance genomics data visualization and

- exploration. *Brief Bioinform.* 2013;14(2):178-192. doi:[10.1093/BIB/BBS017](https://doi.org/10.1093/BIB/BBS017)
25. Myachina F, Bosshardt F, Bischof J, Kirschmann M, Lehner CF. *Drosophila* β -tubulin 97EF is upregulated at low temperature and stabilizes microtubules. *Development.* 2017;144(24):4573-4587. doi:[10.1242/DEV.156109](https://doi.org/10.1242/DEV.156109)
26. Sim NL, Kumar P, Hu J, Henikoff S, Schneider G, Ng PC. SIFT web server: predicting effects of amino acid substitutions on proteins. *Nucleic Acids Res.* 2012;40(W1):W452-W457. doi:[10.1093/NAR/GKS539](https://doi.org/10.1093/NAR/GKS539)
27. Adzhubei IA, Schmidt S, Peshkin L, et al. A method and server for predicting damaging missense mutations. *Nat Methods.* 2010;7(4):248-249. doi:[10.1038/nmeth0410-248](https://doi.org/10.1038/nmeth0410-248)
28. Tanahashi N, Suzuki M, Fujiwara T, et al. Chromosomal localization and immunological analysis of a family of human 26S proteasomal ATPases. *Biochem Biophys Res Commun.* 1998;243(1):229-232. doi:[10.1006/BBRC.1997.7892](https://doi.org/10.1006/BBRC.1997.7892)
29. Karczewski KJ, Francioli LC, Tiao G, et al. The mutational constraint spectrum quantified from variation in 141,456 humans. *Nature.* 2020;581(7809):434-443. doi:[10.1038/s41586-020-2308-7](https://doi.org/10.1038/s41586-020-2308-7)
30. Bedford L, Hay D, Devoy A, et al. Depletion of 26S Proteasomes in mouse brain neurons causes neurodegeneration and Lewy-like inclusions resembling human pale bodies. *J Neurosci.* 2008;28(33):8189-8198. doi:[10.1523/JNEUROSCI.2218-08.2008](https://doi.org/10.1523/JNEUROSCI.2218-08.2008)
31. Fernández-Cruz I, Sánchez-Díaz I, Narváez-Padilla V, Reynaud E. Rpt2 proteasome subunit reduction causes Parkinson's disease like symptoms in *Drosophila*. *IBRO Rep.* 2020;9:65. doi:[10.1016/J.IBROR.2020.07.001](https://doi.org/10.1016/J.IBROR.2020.07.001)
32. Langer CCH, Ejsmont RK, Schö Nbauer C, Schnorrer F, Tomancak P. In vivo RNAi rescue in *Drosophila melanogaster* with genomic transgenes from *Drosophila pseudoobscura*. *PLoS One.* 2010;5(1):e8928. doi:[10.1371/journal.pone.0008928](https://doi.org/10.1371/journal.pone.0008928)
33. Dubiel W, Ferrell K, Pratt G, Rechsteiner M. Subunit 4 of the 26 S protease is a member of a novel eukaryotic ATPase family. *J Biol Chem.* 1992;267(32):22699-22702. doi:[10.1016/S0021-9258\(18\)50002-8](https://doi.org/10.1016/S0021-9258(18)50002-8)
34. Collins GA, Goldberg AL. The logic of the 26S proteasome. *Cell.* 2017;169(5):792-806. doi:[10.1016/J.CELL.2017.04.023](https://doi.org/10.1016/J.CELL.2017.04.023)
35. Cong Tuoc T, Stoykova A. Cell cycle roles of the ubiquitin-proteasome system in neurogenesis. *Cell Cycle.* 2010;16:3174-3180. doi:[10.4161/cc.9.16.12551](https://doi.org/10.4161/cc.9.16.12551)
36. Oikawa T, Sasaki T, Nakamura M, et al. The proteasome is involved in angiogenesis. *Biochem Biophys Res Commun.* 1998;246(1):243-248. doi:[10.1006/BBRC.1998.8604](https://doi.org/10.1006/BBRC.1998.8604)
37. Newberry RW, Raines RT. Secondary forces in protein folding. *ACS Chem Biol.* 2019;14(8):1677-1686. doi:[10.1021/ACSCHEMBIO.9B00339](https://doi.org/10.1021/ACSCHEMBIO.9B00339)
38. Dobson CM. Protein folding and misfolding. *Nature.* 2003;426(6968):884-890. doi:[10.1038/nature02261](https://doi.org/10.1038/nature02261)
39. Nick Pace C, Martin Scholtz J, Grimsley GR. Forces stabilizing proteins. *FEBS Lett.* 2014;588(14):2177-2184. doi:[10.1016/J.FEBSLET.2014.05.006](https://doi.org/10.1016/J.FEBSLET.2014.05.006)
40. Takahashi M, Iwasaki H, Inoue H, Takahashi K. Reverse genetic analysis of the *Caenorhabditis elegans* 26S proteasome subunits by RNA interference. *Biol Chem.* 2002;383(7-8):1263-1266. doi:[10.1515/BC.2002.140/MACHINEREADABLECITATION/RIS](https://doi.org/10.1515/BC.2002.140/MACHINEREADABLECITATION/RIS)
41. Ciechanover A, Brundin P. The ubiquitin proteasome system in neurodegenerative diseases: sometimes the chicken, sometimes the egg. *Neuron.* 2003;40(2):427-446. doi:[10.1016/S0896-6273\(03\)00606-8](https://doi.org/10.1016/S0896-6273(03)00606-8)
42. Rezvani N, Elkharaz J, Lawler K, Mee M, Mayer RJ, Bedford L. Heterozygosity for the proteasomal Psmc1 ATPase is insufficient to cause neuropathology in mouse brain, but causes cell cycle defects in mouse embryonic fibroblasts. *Neurosci Lett.* 2012;521(2):130-135. doi:[10.1016/J.NEULET.2012.05.070](https://doi.org/10.1016/J.NEULET.2012.05.070)
43. Eno CC, Graakjaer J, Svaneby D, et al. 14q32.11 microdeletion including CALM1, TTC7B, PSMC1, and RPS6KA5: a new potential cause of developmental and language delay in three unrelated patients. *Am J Med Genet Part A.* 2021;185(5):1519-1524. doi:[10.1002/AJMG.A.62117](https://doi.org/10.1002/AJMG.A.62117)
44. Gómez-Garre P, Jesús S, Carrillo F, et al. PSMC1 gene in Parkinson's disease. *Eur Neurol.* 2012;68(4):193-198. doi:[10.1159/000339003](https://doi.org/10.1159/000339003)

How to cite this article: Aharoni S, Proskorovski-Ohayon R, Krishnan RK, et al. PSMC1 variant causes a novel neurological syndrome. *Clinical Genetics.* 2022;102(4):324-332. doi:[10.1111/cge.14195](https://doi.org/10.1111/cge.14195)